Simultaneous Optical Performance Monitoring and Modulation Format/Bit-Rate Identification Using Principal Component Analysis

Ming Chieng Tan, Faisal Nadeem Khan, Waled Hussein Al-Arashi, Yudi Zhou, and Alan Pak Tao Lau

***Abstract*—We propose a novel technique for simultaneous multi-impairment monitoring and autonomous bit-rate and modulation format identification (BR-MFI) in next-generation heterogeneous fiber-optic communication networks by using principal component analysis-based pattern recognition on asynchronous delay-tap plots. The results of numerical simulations performed for three commonly used modulation formats at two different bit-rates each demonstrate simultaneous and independent monitoring of optical signal-to-noise ratio, chromatic dispersion, and differential group delay with mean errors of 1 dB, 4 ps/nm, and 1.6 ps, respectively, without knowing the signal's bit-rate and modulation format. Similarly, the results for joint BR-MFI validate accurate identification of all the bit-rates and modulation formats despite the presence of various network impairments. The effects of fiber nonlinearity and transmitter variations on the performance of the proposed technique are also investigated.**

***Index Terms*—Asynchronous delay-tap sampling; Bit-rate and modulation format identification; Optical performance monitoring; Principal component analysis.**

I. Introduction

Optical performance monitoring (OPM) is envisaged to be an integral part of the future dynamic fiber-optic communication networks offering increased flexibility and utilization of available network resources. In dynamic optical networks, each individual wavelength-division-multiplexed (WDM) channel may traverse different paths due to network reconfigurablity enabled by optical add-drop multiplexers and hence, may accumulate different amounts of transmission impairments [1,2]. Therefore, it is imperative to have continuous and real-time information about the extent of channel impairments in dynamic fiber-optic communication networks. Apart from being dynamic, the next-generation optical networks are also envisioned to be heterogeneous in nature incorporating multiple modulation formats as well as different data rates in order to comply with the versatile data rate demands of the end users [3]. Over the past few years, a plethora of OPM techniques capable of monitoring multiple network impairments have been proposed [4–18]. These techniques assume either prior knowledge of the signal's bit-rate and modulation format or the acquisition of this information from the upper-layer protocols. However, for practical purposes, it is not viable to introduce additional cross-layer communication for the sake of OPM at the intermediate network nodes since these nodes can only afford limited complexity. Therefore, there is considerable interest in the development of OPM techniques capable of monitoring multiple impairments for a number of bit-rates and modulation formats without requiring any information about the signal type during the monitoring process.

With the emergence of flexible transceivers, the bit-rates and modulation formats of the signals arriving at the receivers may vary dynamically [19]. Therefore, the digital coherent receivers in future optical networks will be preferred to be capable of autonomous recognition of a transmitted signal's bit-rate and modulation format, for example, for the purpose of selecting an appropriate carrier recovery module among other functionalities. Similarly, bit-rate and modulation format identification (BR-MFI) may also be essential at the intermediate network nodes since the OPM techniques employed may be bit-rate/modulation format dependent. Joint BR-MFI in optical networks is a relatively new area of research and only a few efforts so far have been made toward the realization of this useful feature. In [20–23], modulation format identification (MFI) using digital coherent receivers has been demonstrated. However, these techniques suffer from the following drawbacks. (i) All of these techniques require coherent detection with symbol rate sampling. Since the complexity (and cost) of a full-fledged coherent receiver is quite high, these techniques may not be ideal for use at the intermedi-

Manuscript received October 31, 2013; revised February 14, 2014; accepted March 18, 2014; published April 11, 2014 (Doc. ID 200379).

M. C. Tan and F. N. Khan (e-mail: eefaisal.nadeem@eng.usm.my) are with the School of Electrical and Electronic Engineering, Engineering Campus, Universiti Sains Malaysia, Penang, Malaysia.

W. H. Al-Arashi is with the Department of Electronic Engineering, University of Science and Technology, Sana'a, Yemen.

Y. Zhou is with the Department of Electrical and Computer Engineering, Texas A&M University, College Station, Texas 77843, USA.

A. P. T. Lau is with the Photonics Research Centre, The Hong Kong Polytechnic University, Kowloon, Hong Kong, China.

http://dx.doi.org/10.1364/JOCN.6.000441

ate network nodes. (ii) Almost all of these techniques are limited to MFI only and cannot enable joint BR-MFI. Recently, we proposed artificial neural network (ANN)-based techniques for MFI [24] as well as joint BR-MFI [25] in heterogeneous fiber-optic networks with good identification accuracies. However, both of these techniques focus on identifying the type of the signal and do not provide any information about the quality of the signal.

In this paper, we extend our previous work and propose a cost-effective technique which employs principal component analysis (PCA)-based pattern recognition in combination with asynchronous delay-tap plots (ADTPs) for monitoring multiple network impairments for several different modulation formats and data rates without necessitating hardware changes and without requiring any information about the signal type during the online monitoring process. The proposed technique can also accurately identify the bit-rate and modulation format of the signal from a known set of bit-rates and modulation formats. To demonstrate the validity of the proposed technique, numerical simulations are performed for 10/20 Gbps return-to-zero (RZ) on–off keying (OOK), 40/100 Gbps polarization-multiplexed (PM) RZ quadrature phase-shift keying (QPSK), and 100/200 Gbps PM non-return-to-zero (NRZ) 16 quadrature amplitude modulation (16QAM) signals. The results show simultaneous and independent optical signal-to-noise ratio (OSNR), chromatic dispersion (CD), and differential group delay (DGD) monitoring as well as joint BR-MFI with good accuracies.

II. Joint OPM and BR-MFI Using PCA

Figure 1 shows ADTPs for three modulation formats at two different bit-rates in the presence of various transmission impairments. An ADTP is quintessentially a two-dimensional (2D) histogram of closely located sample pairs with the advantage that its generation does not require timing/clock information unlike the conventional synchronous eye diagrams [6,7]. It is evident from Fig. 1 that the patterns reflected by the ADTPs are sensitive to network impairments as well as to the type of signal. Therefore, statistical pattern recognition techniques can be used to exploit the ADTPs' features for joint multi-impairment monitoring and BR-MFI. Recently, several ADTP-based multi-impairment monitoring techniques have been proposed [5,8–10]. However, all these techniques essentially require information about the actual bit-rate and modulation format of the signal for the purpose of selecting a predictor or a calibration curve appropriate for that specific signal type and cannot independently perform BR-MFI. In this work, we treat ADTPs as images (called ADTP-images) and analyze their characteristics using PCA, also known as the Karhunen–Loève transform (KLT), which is a statistical technique for data representation and features extraction [26,27]. Given a set of images represented in a high-dimension image space, PCA finds a small set of orthonormal eigenvectors spanning a subspace so that all the given images can be represented without losing much information [28,29]. Thus, PCA can reduce the dimensionality of an image space, resulting in a much more compact representation of the images.

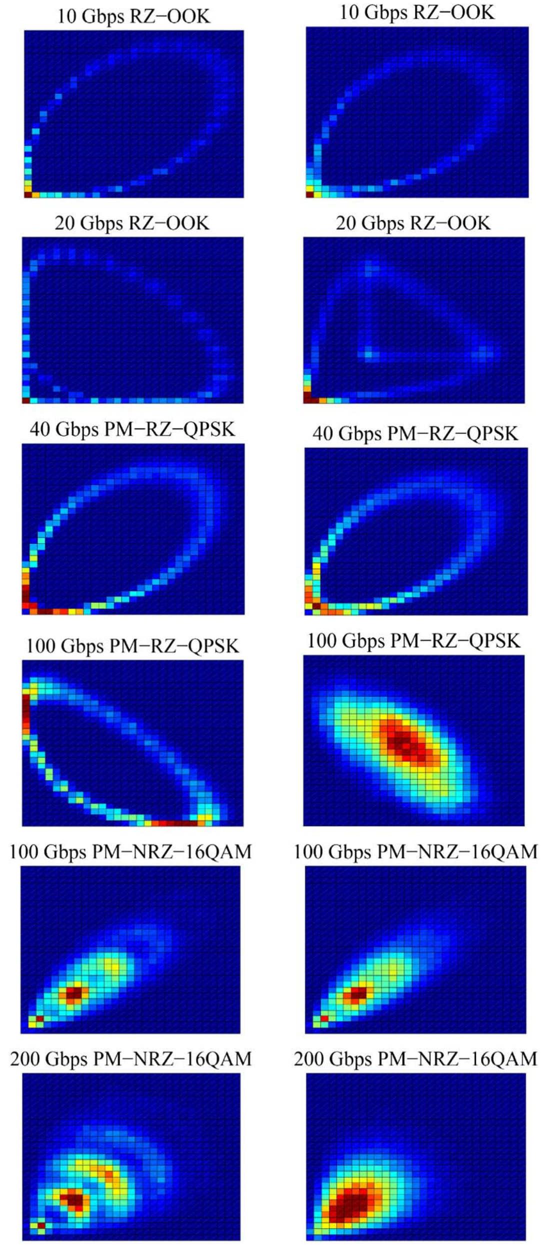

Fig. 1. ADTPs for three modulation formats at two different bit-rates for various combinations of impairments. The left column corresponds to OSNR = 20 dB and without CD and DGD, whereas the right column corresponds to OSNR = 18 dB, CD = 100 ps/nm, and DGD = 5 ps ($\alpha = 45°$). A tap-delay of 15 ps is used for the generation of all ADTPs.

Consider a set S having M ADTP-images corresponding to various known combinations of impairments, bit-rates, and modulation formats. Let the size of each ADTP-image be $N \times N$. An ADTP-image can also be expressed as a one-dimensional vector x_i of length N^2 by concatenating all the columns (or rows) of the image. Hence, we can represent the whole set S by one big image matrix

$X = [x_1, x_2, \ldots, x_M]$ of size $N^2 \times M$. The mean image vector Ψ of matrix X is defined as

$$\Psi = \frac{1}{M}\sum_{i=1}^{M} x_i. \tag{1}$$

Subtracting Ψ from each column of the matrix X, we obtain a zero-mean image matrix $Y = [y_1, y_2, \ldots, y_M]$. The covariance matrix C of Y is given as

$$C = \frac{1}{M}\sum_{i=1}^{M} y_i y_i^T = YY^T. \tag{2}$$

The size of matrix $C = YY^T$ is $N^2 \times N^2$ and hence, it can have up to N^2 eigenvectors and eigenvalues. Let v_i and λ_i be the ith eigenvector and eigenvalue of C, respectively; then by using

$$Cv_i = \lambda_i v_i \quad \text{for} \quad i = 1, 2, \ldots, N^2 \tag{3}$$

we can determine N^2 eigenvectors, also called principal components (PCs), of C. The computed eigenvectors are ranked according to their eigenvalues and amongst them K (where $K \ll N^2$) eigenvectors corresponding to the K largest eigenvalues are selected while the rest are discarded. The value of K is chosen such that the following criterion is satisfied:

$$R = \sum_{i=1}^{K} \lambda_i \Big/ \sum_{i=1}^{N^2} \lambda_i > P, \tag{4}$$

where the value of P is typically chosen to be above 0.9 [26,27]. The selected eigenvectors span a K-dimensional subspace of the original N^2-dimensional image space. Any vector y can be approximated as a weighted-sum of the selected eigenvectors in this subspace, i.e.,

$$y \approx \sum_{k=1}^{K} w_k v_k \Rightarrow w_k = v_k^T y \quad \text{for} \quad k = 1, 2, \ldots, K. \tag{5}$$

The weights w_k constitute a vector $\Omega = [w_1, w_2, \ldots, w_K]^T$, called the feature vector of the ADTP-image. Thus, using Eq. (5), we can compute the feature vectors of all the ADTP-images in S. These feature vectors can then be used to construct a reference database for subsequent image recognition purposes.

In order to estimate the unknown impairment values as well as to identify the bit-rate and modulation format corresponding to a given ADTP-image, we can compute its feature vector Ω (using K eigenvectors obtained for the set S) and compare it with all the available feature vectors in the reference database to determine which feature vector amongst all best matches with the given feature vector. This can be accomplished by finding the minimum Euclidean distance $D_{\min}$ between the feature vector Ω of the given ADTP-image and all the other feature vectors in the reference database, i.e.,

$$D_{\min} = \min(\|\Omega - \Omega_j\|_{j=1,2,\ldots,M}), \tag{6}$$

where Ω_j is the feature vector of the jth ADTP-image in the reference database. The use of extremely reduced size feature vectors, obtained using PCA, makes the feature vector matching process computationally efficient, which is advantageous especially for real-time applications. To further reduce the computational complexity of the feature vectors matching process, a threshold value θ for the Euclidean distance $D_j = \|\Omega - \Omega_j\|_{j=1,2,\ldots,M}$ can be defined and the matching process is aborted as soon as $D_j \leq \theta$. This approach (also used in automatic face recognition systems) requires a careful selection of θ so as to reduce the computational complexity and time while maintaining the desired estimation accuracy [28,29]. The impairment values, bit-rate, and modulation format corresponding to the feature vector in the reference database, which best matches with the given feature vector Ω, are taken as the estimated impairment values and the identified bit-rate and modulation format.

III. System Configuration and Results

In order to analyze the validity of the proposed technique, we have performed numerical simulations using the VPI software [30]. Figure 2 shows the system configuration used in our simulations. Six different transmitters are used to generate 10/20 Gbps RZ-OOK, 40/100 Gbps

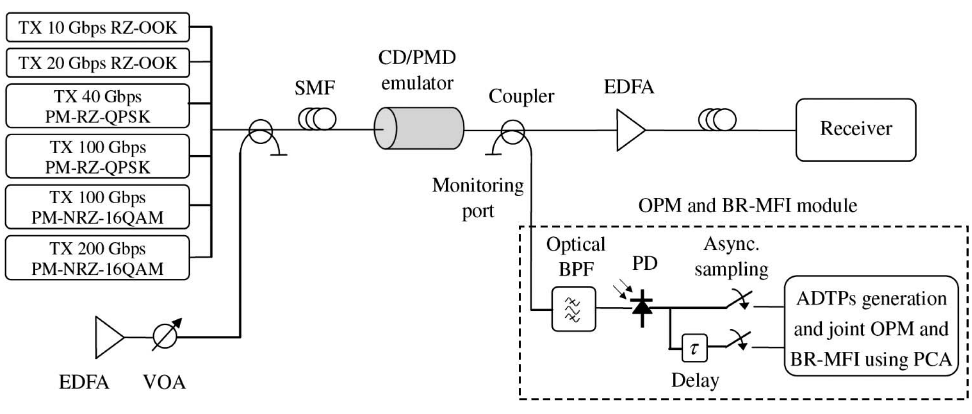

Fig. 2. System setup for joint OPM and BR-MFI using PCA and ADTPs.

PM-RZ-QPSK, and 100/200 Gbps PM-NRZ-16QAM signals, which are then transmitted over a single-mode fiber (SMF). For PM signals, we assume the same bit-rates for the signals in two polarizations. Furthermore, the two orthogonally polarized signals are assumed to be initially time-aligned with each other. The OSNRs of the signals are varied in the range of 14–28 dB (in steps of 2 dB) by using an erbium-doped fiber amplifier (EDFA) with a variable optical attenuator (VOA) in front. A CD emulator is used to add CD in the range of −500–500 ps/nm in steps of 80 ps/nm while a polarization-mode dispersion (PMD) emulator is utilized to introduce DGD in the range of 0–10 ps in steps of 2 ps. To simulate the random PMD effects in real optical fibers, the angle α between the transmitted signal's state of polarization (SOP) and the principal states of polarization (PSP) of the PMD emulator is altered at random. For each specific value of DGD, seven random values of α between 0° and 90° are considered. A fraction of the optical signal (i.e., a fixed power level of −6 dBm) is tapped from the link with the help of an optical coupler and is fed into the monitoring module where an optical band-pass filter (BPF) is used to filter the desired channel. The filtered optical signal is then directly detected using a receiver with optical and electrical bandwidths of 0.8 nm and 50 GHz, respectively. The electrical signal after optical-to-electronic (O/E) conversion is sampled (with a sampling rate of 500 Msamples/s) using asynchronous delay-tap sampling (ADTS) with a tap-delay of 15 ps. There is no rule of thumb for choosing the tap-delay in ADTS and often a tap-delay that is just a fraction (i.e., from 1/10 to 1/4) of the symbol period is used [5–9]. Since the maximum and minimum symbol periods for the bit-rates and modulation formats considered in this work are 100 and 40 ps, respectively, we have selected a tap-delay of 15 ps in this case. Another reason for the selection of this tap-delay is that the ADTP patterns (for the set of signals involved) resulting from this tap-delay are visibly well distinguishable, as is clear from Fig. 1. In general, the tap-delay can be adjusted by starting with a fraction of the minimum symbol period amongst all the signals under consideration and then varying it iteratively until the required estimation accuracy is attained. A total of 100,000 delay-tap sample pairs are collected and used to generate an ADTP with 30×30 bins. A large data set consisting of 26,208 ADTPs corresponding to different OSNR, CD, DGD, α, bit-rates, and modulation formats is obtained. Two distinct subsets called reference and testing data sets are then generated by randomly dividing the ADTPs in the overall data set into two parts. Next, PCA is applied to compute the feature vectors of all the ADTP-images in the reference data set. Figure 3(a) shows the eigenvalues for a few PCs in descending order. It is evident from the figure that the eigenvalues rapidly converge to zero. Figure 3(b) shows the value of parameter R as a function of the number of PCs selected K. It is clear from the figure that the value of R is above 0.98 for just eight PCs (out of a total of 900 PCs). This implies that it is reasonable to use only a few PCs for the synthesis of feature vectors and discard the remaining without losing much information. The feature vectors corresponding to

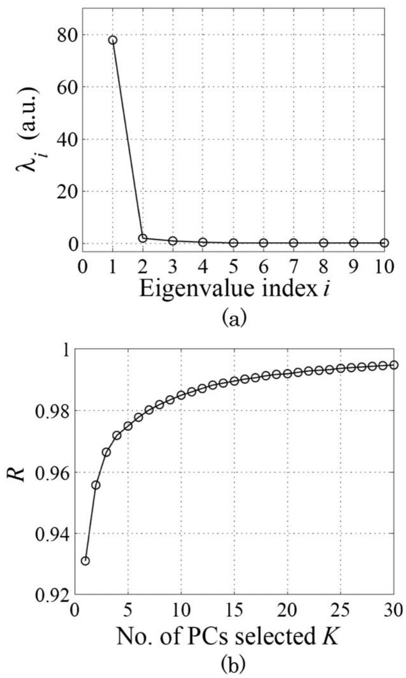

Fig. 3. (a) Eigenvalues λ_i for a few PCs in descending order. (b) Parameter R as a function of the number of PCs selected.

the ADTP-images in the reference data set are used to construct a reference database for subsequent image recognition.

To investigate the performance of the proposed technique, feature vectors of all the ADTP-images in the testing data set are determined. For each feature vector in the testing data set, the best match in the reference database is obtained using the procedure described in the previous section, and the OSNR, CD, DGD, bit-rate, and modulation format are then determined accordingly. Figure 4 shows the results of OSNR, CD, and DGD monitoring for three different proportions, i.e., 70%:30%, 60%:40%, and 50%:50%, of the reference and testing data sets. Since the size of the overall data set is fixed, i.e., 26,208, the three different proportions of the reference and testing data sets essentially mean three different sizes of the reference database, i.e., 18,346, 15,724, and 13,104. Note that since the overall data set encompasses an equal number of ADTP-images (i.e., $26,208/6 = 4368$) for all six signal types under consideration and since the testing data set is obtained by randomly selecting 30%, 40%, and 50% of the ADTP-images in the overall data set, the testing data set will contain an approximately equal number of ADTP-images (and thus feature vectors) for each signal type. It is clear from Fig. 4 that the estimation accuracy depends on the number of PCs selected up to a certain point. For 10 PCs, the mean estimation errors for OSNR, CD, and DGD are 1 dB, 4 ps/nm, and 1.6 ps, respectively. It is also evident from the figure that a reduction in the size of the reference database, i.e., from 70% to 50% of the overall data, does not result in a significant increase in estimation errors.

Table I summarizes the results of joint BR-MFI using only two as well as more than two PCs. The identification accuracies given in Table I are calculated by dividing the number of correct identifications for a given bit-rate and modulation format with the total number of feature vectors corresponding to that signal type in the testing data set. Thus, an identification accuracy of 100%, for example, would signify no errors encountered in identifying that signal type. It is evident from the table that good identification accuracies are achieved for all six signal types under consideration with an overall accuracy (i.e., average of the accuracies for the six signal types) of 92.6% using only two PCs and 100% for more than two PCs, thus validating the applicability of the proposed technique. The identification accuracies demonstrated by the proposed technique are better than the ones shown by the ANN-based BR-MFI technique [25]. Figure 5 shows the effect of the number of PCs selected on the overall identification accuracy. It is clear from the figure that using only one PC, the identification accuracy is merely 70%, while using three and more PCs, the accuracy readily approaches 100%. Note that all these high identification accuracies have been achieved in practical channel conditions, i.e., in the presence of various transmission impairments. It is also evident from Fig. 5 that the identification accuracy is not affected by the size of the reference database.

To analyze the reliability of the proposed technique against variations that may exist between transmitters (even among the ones belonging to the same model), for example, due to manufacturing tolerances and components ageing, we have performed numerical simulations by utilizing transmitters for the generation of testing data which are dissimilar to the ones used for the synthesis of the reference database. In particular, the rise and fall times

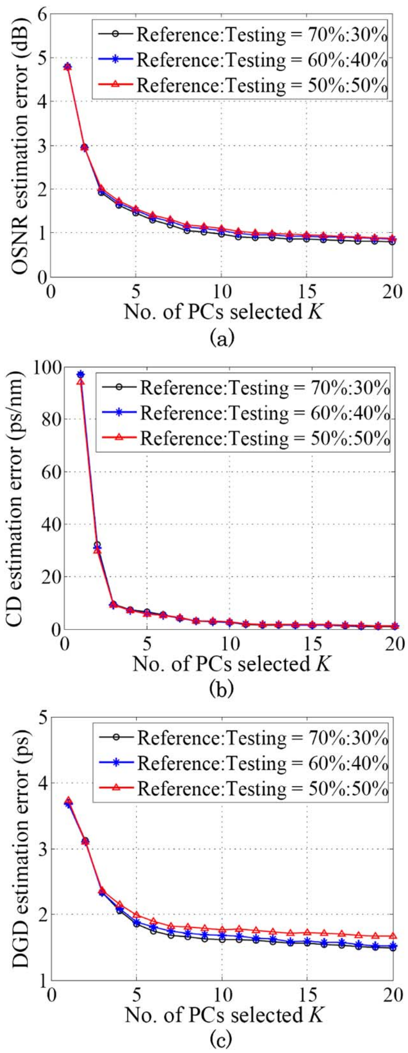

Fig. 4. Mean estimation error for (a) OSNR, (b) CD, and (c) DGD as a function of number of PCs selected for three different proportions of reference and testing data. The total number of reference and testing data is 26,208.

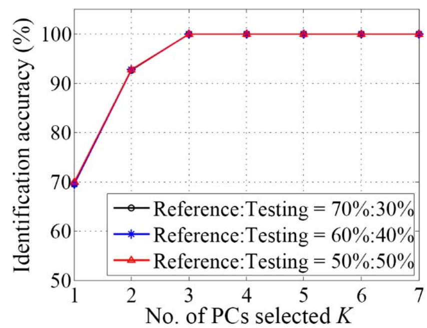

Fig. 5. Effect of number of PCs selected on the overall identification accuracy for three different proportions of reference and testing data.

TABLE I
IDENTIFICATION ACCURACIES FOR VARIOUS BIT-RATES AND MODULATION FORMATS USING ONLY TWO PCS (NORMAL) AND MORE THAN TWO PCS (BOLD)[a]

	Identified Bit-Rate and Modulation Format					
Actual Bit-Rate and Modulation Format	10 Gbps RZ-OOK	20 Gbps RZ-OOK	40 Gbps PM-RZ-QPSK	100 Gbps PM-RZ-QPSK	100 Gbps PM-NRZ-16QAM	200 Gbps PM-NRZ-16QAM
10 Gbps RZ-OOK	98.05% **100%**	1.95%	–	–	–	–
20 Gbps RZ-OOK	1.81%	98.19% **100%**	–	–	–	–
40 Gbps PM-RZ-QPSK	–	–	98.45% **100%**	0.93%	–	0.62%
100 Gbps PM-RZ-QPSK	–	–	1.51%	93.41% **100%**	3.79%	1.29%
100 Gbps PM-NRZ-16QAM	–	–	–	2.76%	83.28% **100%**	13.95%
200 Gbps PM-NRZ-16QAM	–	–	0.39%	0.94%	14.47%	84.2% **100%**

[a]The overall identification accuracy is 92.6% for two PCs and 100% for more than two PCs.

of the pulses generated by the two sets of transmitters differ in the range of 15%–25%. Similarly, the extinction ratios of the two sets of transmitters differ by 3 dB. Figure 6 shows the results of OSNR, CD, and DGD monitoring, as well as overall identification accuracy, for this scenario. It is clear from the figure that mean CD estimation error and identification accuracy remain almost unaffected while using dissimilar transmitters for the generation of reference database and testing data. Though the mean estimation errors for OSNR and DGD are increased, i.e., 1.4 dB and 2.4 ps (for 10 PCs), respectively, they still remain within tolerable limits. This implies that the proposed technique is resilient against variations in transmitter characteristics. To make the technique more robust against transmitter variations, the reference database may be synthesized by employing a number of dissimilar transmitters with different pulse characteristics.

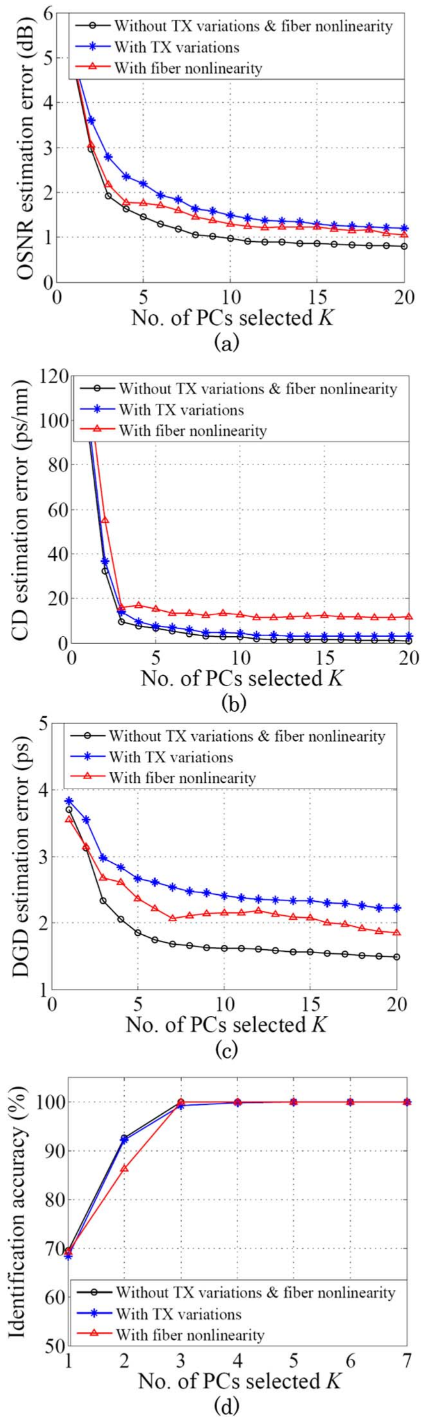

Fig. 6. Effect of transmitter variations and fiber nonlinearity on (a) OSNR estimation, (b) CD estimation, (c) DGD estimation, and (d) overall identification accuracy for a 70%:30% proportion of reference and testing data. The total number of reference and testing data is 26,208.

Finally, we have investigated the performance of the proposed technique in the presence of fiber nonlinearity, whereby the reference database is generated considering three transmission impairments, i.e., noise, CD, and DGD while the testing data are also affected by the fiber nonlinear effects. The transmission link used in our simulations is 1000 km long and consists of multiple spans of fiber with span length of around 60 km. The input power and fiber nonlinear coefficient γ are 0 dBm and $1.2/\mathrm{W}\cdot\mathrm{km}$, respectively. The simulation results are shown in Fig. 6. It is clear from Figs. 6(a)–6(c) that the mean estimation errors for OSNR, CD, and DGD are slightly increased in the presence of fiber nonlinearity and are approximately 1.2 dB, 12 ps/nm, and 2.1 ps (for 10 PCs), respectively. On the other hand, it is evident from Fig. 6(d) that the identification accuracy remains almost unchanged. If a reduction in estimation errors, caused by the fiber nonlinear effects, is desired, then this can be potentially achieved by also including the feature vectors corresponding to several different values of γ and link lengths in the reference database.

IV. Discussion

During the synthesis of the reference database, the proposed technique indeed requires information about various signal types existing in the network. However, the reference database is generated offline and prior to the online monitoring process. We would like to emphasize that all the existing ADTP as well as asynchronous amplitude histogram (AAH)-based OPM techniques also require this prior information, for example, for the training of a predictor [10] or for the acquisition of the calibration curves [8,9,11,16–18]. However, the main drawback of all these techniques is that they also require precise knowledge of the signal type during the actual online monitoring process for the purpose of selecting an appropriate predictor or a calibration curve. In contrast, the proposed technique does not require this information during the online monitoring process and can autonomously identify the signal type as long as it belongs to a specific set of signals considered during the construction of the reference database.

In this work, we have considered OSNR, CD, and DGD in the ranges of 14–28 dB, −500–500 ps/nm, and 0–10 ps, respectively, because these impairment ranges are typically experienced in practical dispersion-compensated optical networks. The estimation accuracies for both multi-impairment monitoring and BR-MFI are anticipated to be relatively less if the impairments exceed these ranges. This is because the proposed technique relies on the fact that the ADTP patterns obtained for various impairment values as well as for different bit-rates and modulation formats are distinguishable from each other. However, this condition is valid up to certain ranges of impairments. For large transmission impairments, the signal pulses are extremely distorted, and consequently, the ADTP patterns are not well distinguishable. This puts a limit on the allowed ranges of transmission impairments for the proposed as well as other ADTP-based techniques [5,7–12]. Note that by utilizing simple direct detection along with ADTS, the proposed technique primarily aims for dispersion-compensated optical networks (having a considerable amount of residual CD). However, it may potentially be used in dispersion-uncompensated fiber-optic networks by employing coherent detection instead, whereby first a coarse CD compensation can be performed blindly and adaptively [23], and afterward, the proposed technique can be used for the precise estimation of residual CD as well as other critical transmission parameters.

V. Conclusions

In this paper, we proposed a PCA-based technique for simultaneous OSNR, CD, and PMD monitoring for several commonly used modulation formats and data rates with good monitoring accuracies and without requiring any information about the signal type during the online monitoring process. The proposed technique can also accurately identify the bit-rates and modulation formats of the signals despite the presence of noise, CD, and PMD. The effects of transmitter variations and fiber nonlinearity on the estimation accuracy of proposed technique are also investigated and the tolerances are examined. Due to its simplicity, this technique can be used in receivers as well as at the intermediate network nodes in future high-speed dynamic optical networks.

Acknowledgments

This work was supported by the Research University Individual grant (1001/PELECT/814203) and Short-term grant (304/PELECT/60313004) of the Universiti Sains Malaysia.

References

[1] D. C. Kilper, R. Bach, D. Blumenthal, D. Einstein, T. Landolsi, L. Ostar, M. Preiss, and A. E. Willner, "Optical performance monitoring," *J. Lightwave Technol.*, vol. 22, no. 1, pp. 294–304, Jan. 2004.

[2] Z. Pan, C. Yu, and A. E. Willner, "Optical performance monitoring for the next generation optical communication networks," *Opt. Fiber Technol.*, vol. 16, no. 1, pp. 20–45, Jan. 2010.

[3] A. Nag, M. Tornatore, and B. Mukherjee, "Optical network design with mixed line rates and multiple modulation formats," *J. Lightwave Technol.*, vol. 28, no. 4, pp. 466–475, Feb. 2010.

[4] A. E. Willner, Z. Pan, and C. Yu, "Optical performance monitoring," in *Optical Fiber Telecommunications VB*, I. P. Kaminow, T. Li, and A. E. Willner, Eds. Academic, 2008, ch. 7.

[5] C. K. Chan, *Optical Performance Monitoring*. Academic, 2010.

[6] S. D. Dods and T. B. Anderson, "Optical performance monitoring technique using delay tap asynchronous waveform sampling," in *Proc. Optical Fiber Communication Conf. (OFC)*, Anaheim, CA, Mar. 2006, paper OThP5.

[7] F. N. Khan, A. P. T. Lau, Z. Li, C. Lu, and P. K. A. Wai, "Statistical analysis of optical signal-to-noise ratio monitoring using delay-tap sampling," *IEEE Photon. Technol. Lett.*, vol. 22, no. 3, pp. 149–151, Feb. 2010.

[8] B. Kozicki, A. Maruta, and K. Kitayama, "Transparent performance monitoring of RZ-DQPSK systems employing delay-tap sampling," *J. Opt. Netw.*, vol. 6, no. 11, pp. 1257–1269, Nov. 2007.

[9] B. Kozicki, A. Maruta, and K. Kitayama, "Experimental investigation of delay-tap sampling technique for online monitoring of RZ-DQPSK signals," *IEEE Photon. Technol. Lett.*, vol. 21, no. 3, pp. 179–181, Feb. 2009.

[10] T. B. Anderson, A. Kowalczyk, K. Clarke, S. D. Dods, D. Hewitt, and J. C. Li, "Multi impairment monitoring for optical networks," *J. Lightwave Technol.*, vol. 27, no. 16, pp. 3729–3736, Aug. 2009.

[11] Z. Li, Z. Jian, L. Cheng, Y. Yang, C. Lu, A. P. T. Lau, C. Yu, H. Y. Tam, and P. K. A. Wai, "Signed chromatic dispersion monitoring of 100 Gbit/s CS-RZ DQPSK signal by evaluating the asymmetry ratio of delay tap sampling," *Opt. Express*, vol. 18, no. 3, pp. 3149–3157, Feb. 2010.

[12] F. N. Khan, A. P. T. Lau, Z. Li, C. Lu, and P. K. A. Wai, "OSNR monitoring for RZ-DQPSK systems using half-symbol delay-tap sampling technique," *IEEE Photon. Technol. Lett.*, vol. 22, no. 11, pp. 823–825, June 2010.

[13] X. Wu, J. A. Jargon, R. A. Skoog, L. Paraschis, and A. E. Willner, "Applications of artificial neural networks in optical performance monitoring," *J. Lightwave Technol.*, vol. 27, no. 16, pp. 3580–3589, Aug. 2009.

[14] L. Cheng, Z. Li, C. Lu, A. P. T. Lau, H. Y. Tam, and P. K. A. Wai, "Chromatic dispersion monitoring based on variance of received optical power," *IEEE Photon. Technol. Lett.*, vol. 23, no. 8, pp. 486–488, Apr. 2011.

[15] K. K. Qureshi, Z. Jian, C. Lu, H. Y. Tam, and P. K. A. Wai, "Tunable polarization maintaining fiber Bragg grating based OSNR monitor," *Opt. Fiber Technol.*, vol. 16, no. 4, pp. 222–224, June 2010.

[16] A. P. T. Lau, Z. Li, F. N. Khan, C. Lu, and P. K. A. Wai, "Analysis of signed chromatic dispersion monitoring by waveform asymmetry for differentially-coherent phase-modulated systems," *Opt. Express*, vol. 19, no. 5, pp. 4147–4156, Feb. 2011.

[17] Z. Li and G. Li, "Chromatic dispersion and polarization-mode dispersion monitoring for RZ-DPSK signals based on asynchronous amplitude-histogram evaluation," *J. Lightwave Technol.*, vol. 24, no. 7, pp. 2859–2866, July 2006.

[18] B. Kozicki, O. Takuya, and T. Hidehiko, "Optical performance monitoring of phase-modulated signals using asynchronous amplitude histogram analysis," *J. Lightwave Technol.*, vol. 26, no. 10, pp. 1353–1361, May 2008.

[19] K. Roberts and C. Laperle, "Flexible transceivers," in *Proc. European Conf. on Optical Communication (ECOC)*, Amsterdam, Sept. 2012, paper We.3.A.3.

[20] N. G. Gonzalez, D. Zibar, and I. T. Monroy, "Cognitive digital receiver for burst mode phase modulated radio over fiber links," in *Proc. European Conf. on Optical Communication (ECOC)*, Turin, Sept. 2010, paper P6.11.

[21] R. Borkowski, D. Zibar, A. Caballero, V. Arlunno, and I. T. Monroy, "Optical modulation format recognition in Stokes space for digital coherent receivers," in *Proc. Optical Fiber Communication Conf. (OFC)*, Anaheim, CA, Mar. 2013, paper OTh3B.3.

[22] R. Borkowski, D. Zibar, A. Caballero, V. Arlunno, and I. T. Monroy, "Stokes space-based optical modulation format recognition for digital coherent receivers," *IEEE Photon. Technol. Lett.*, vol. 25, no. 21, pp. 2129–2132, Nov. 2013.

[23] P. Isautier, A. Stark, K. Mehta, R. DeSalvo, and S. E. Ralph, "Autonomous software-defined coherent optical receivers," in *Proc. Optical Fiber Communication Conf. (OFC)*, Anaheim, CA, Mar. 2013, paper OTH3B.4.

[24] F. N. Khan, Y. Zhou, A. P. T. Lau, and C. Lu, "Modulation format identification in heterogeneous fiber-optic networks using artificial neural networks," *Opt. Express*, vol. 20, no. 11, pp. 12422–12431, May 2012.

[25] F. N. Khan, Y. Zhou, Q. Sui, and A. P. T. Lau, "Non-data-aided joint bit-rate and modulation format identification for next-generation heterogeneous optical networks," *Opt. Fiber Technol.*, vol. 20, no. 2, pp. 68–74, Mar. 2014.

[26] I. T. Jolliffe, *Principal Component Analysis*, 2nd ed. Springer, 2002.

[27] J. E. Jackson, *A User's Guide to Principal Components*. Wiley, 2003.

[28] M. Turk and A. Pentland, "Eigenfaces for recognition," *J. Cogn. Neurosci.*, vol. 3, no. 1, pp. 71–86, Mar. 1991.

[29] M. Turk and A. Pentland, "Face recognition using eigenfaces," in *Proc. IEEE Conf. on Computer Vision and Pattern Recognition*, Maui, HI, June 1991, pp. 586–591.

[30] VPIsystems, "VPItransmissionMaker."